ELSEVIER

Thin-Walled Structures 40 (2002) 925–953

THIN-WALLED STRUCTURES

www.elsevier.com/locate/tws

A simplified method for elastic large deflection analysis of plates and stiffened panels due to local buckling

Eirik Byklum *, Jørgen Amdahl

Department of Marine Structures, Norwegian University of Science and Technology, N-7491 Trondheim, Norway

Received 31 October 2001; received in revised form 13 May 2002; accepted 28 May 2002

Abstract

A computational model for analysis of local buckling and postbuckling of stiffened panels is derived. The model provides a tool that is more accurate than existing design codes, and more efficient than nonlinear finite element methods. Any combination of biaxial in-plane compression or tension, shear, and lateral pressure may be analysed. Deflections are assumed in the form of trigonometric function series. The deformations are coupled such that continuity of rotation between the plate and the stiffener web is ensured, as well as longitudinal continuity of displacement. The response history is traced using energy principles and perturbation theory. The procedure is semi-analytical in the sense that all energy formulations are derived analytically, while a numerical method is used for solving the resulting set of equations, and for incrementation of the solution. The stress in certain critical points are checked using the von Mises yield criterion, and the onset of yielding is taken as an estimate of ultimate strength for design purposes.

Keywords: Stiffened panel; Local model; Buckling; Postbuckling; Ultimate strength; Large deflection plate theory; Energy principles

* Corresponding author. Tel.: +47-73-59-55-37; fax: +47-73-59-55-28.
E-mail address: eirikby@marin.ntnu.no (E. Byklum).

0263-8231/02/$ - see front matter.
PII: S0263-8231(02)00042-3

1. Introduction

Stiffened plates are extensively used in steel and aluminum structures such as ships and offshore installations. The buckling characteristics of such panels are of crucial importance for the overall structural strength. The post-buckling behavior is especially important because of the reserve capacity which exists after the initial buckling. It is usual to accept that local buckling of plate members may take place, but overall stiffener or grillage buckling should not occur. The column approach is often used for buckling assessment in design codes, such as the DNV Classification Note for Buckling Strength Analysis [1]. These formulations have the advantage of being relatively simple, and provide quick strength estimates. However, looking at the deflection behavior of actual stiffened panels, it is clear that a column model does not provide the best representation of the real structural response. Usually, local deformations dominate, while lateral deflection in the global mode is less significant.

Although hand calculations using explicit design formulas have been important in the ship building industry, computational tools are becoming more and more common. The need for explicit formulas is therefore decreasing. Nonlinear finite element analysis (FEM) of stiffened panels is not practical for design purposes due to the cost of modeling and computing. The approach presented in the following is a compromise between simple design formulations and more accurate, but also more time consuming, FEM analysis. It provides a tool for faster analysis, and gives more information regarding deformation modes and load–response characteristics.

Previous work in the field of analytic or semi-analytic buckling formulations have been restricted mostly to linearized buckling predictions, neglecting non-linear geometrical effects in the large deflection region, such as [2,3]. Some work has been performed on the large deflection response of unstiffened plates [4,5]. In the present work, the coupled behavior of a plate with an attached stiffener is treated using large deflection theory for both the plate and the stiffener.

2. Problem formulation

The stiffened panel is assumed to consist of a rectangular plate area with longitudinal stiffeners in one direction and heavy transverse girders in the other direction, as shown in Fig. 1. This is a typical configuration for the deck, side or bottom of a ship hull girder. The stiffener may be a flat bar, angle bar, tee bar or bulb bar. Only local buckling is considered, which means that no overall deflection of the panel is assumed to occur. A stiffener with attached plating may therefore be considered as representative for a whole stiffened panel.

The loads acting on a stiffened panel in a ship are in-plane compression or tension, resulting from the overall hull girder bending moment or torsion, shear force resulting from the hull girder shear force, and lateral pressure resulting from internal cargo or the external sea. The shear force and lateral pressure are assumed to have a constant value over the length and breadth of the plate, while the in-plane compression or tension is assumed to be linearly varying.

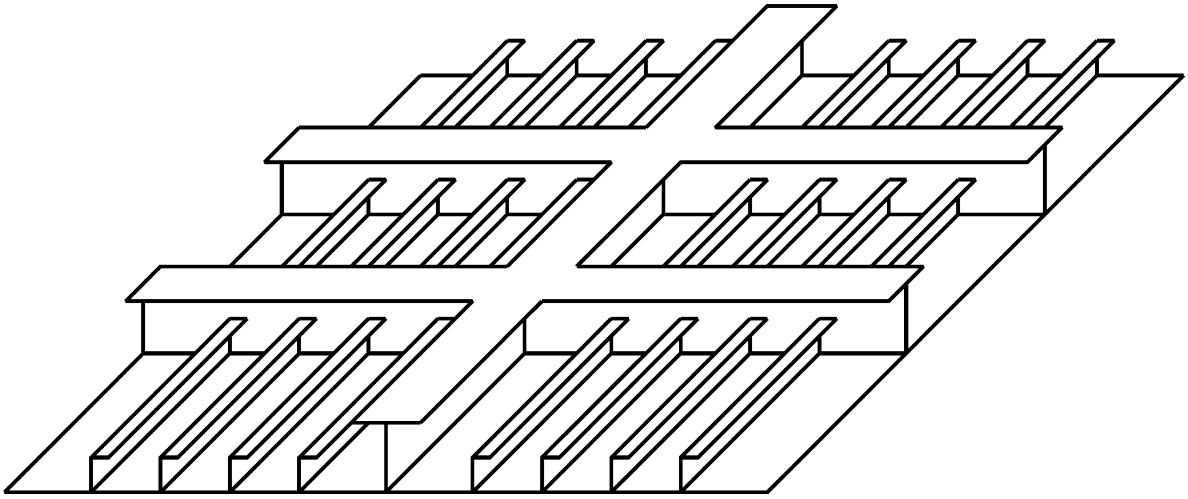

Fig. 1. Stiffened panel.

The response of the stiffened plate during buckling is studied using the principle of minimum potential energy. The aim is to trace the complete load-deflection equilibrium curve in the prebuckling and postbuckling region, and provide estimates of the ultimate load and deformation. Geometrical nonlinearities are accounted for using large deflection plate theory. The formulations developed may be called semi-analytical. The energy equations are integrated analytically, and stiffness coefficients are obtained explicitly. However, a numerical method is used for solving the equation system.

2.1. The principle of minimum potential energy

The principle of minimum potential energy states that 'of all the possible deflections satisfying kinematic compatibility, those which satisfy static equilibrium will give a stationary value of the potential energy of the body'[6]:

$$\delta\Pi = \delta U + \delta T = 0 \tag{1}$$

where Π is total potential energy, U is internal energy, T is potential of external loads, and δ is the variational operator. The principle is valid for conservative systems, which means that the material must be elastic.

In the Rayleigh–Ritz method, the continuous displacement of a body is represented by a set of assumed displacement functions. The problem is reduced to finding the unknown coefficients, or amplitudes, of these functions. It is required that the assumed functions satisfy the essential but not necessarily the natural boundary conditions. The method is often used with the principle of minimum potential energy. For instance, assuming that the displacement can be written as

$$w(x,y) = \sum_{m=1}^{M} \sum_{n=1}^{N} A_{mn} g_m(x) g_n(y) \tag{2}$$

the principle of minimum potential energy can be reformulated using the Rayleigh–Ritz method to:

$$\frac{\partial \Pi}{\partial A_{mn}} = 0 \tag{3}$$

This formulation reduces the problem to finding the unknown amplitudes A_{mn}.

2.2. Large deflection plate theory

Using the Love–Kirchoff assumption that lines normal to the undeformed middle surface remain normal to this surface, the strains in a material point is taken as the sum of membrane strain and bending strain:

$$\varepsilon_{ij}^{\text{tot}} = \varepsilon_{ij} - zw_{ij} \qquad i,j = x,y \tag{4}$$

where z is the vertical distance from the plate neutral axis to the material point in consideration. According to Marguerre [7], who extended the von Kármán nonlinear plate theory to plates with an initial curvature, the membrane strains can be written as:

$$\varepsilon_x = u_x + \frac{1}{2}w_x^2 + w_{0,x}w_x \tag{5}$$

$$\varepsilon_y = v_y + \frac{1}{2}w_y^2 + w_{0,y}w_y \tag{6}$$

$$\gamma_{xy} = u_y + v_x + w_xw_y + w_{0,x}w_y + w_xw_{0,y} \tag{7}$$

where w and w_0 are the additional and initial out-of-plane deflection of the plate, respectively.

Static equilibrium is achieved through the plate differential equation. Introducing the Airy stress function F, defined so that

$$\sigma_x = F_{yy} \tag{8}$$

$$\sigma_y = F_{xx} \tag{9}$$

$$\sigma_{xy} = -F_{xy} \tag{10}$$

the differential equation can be written as [8]

$$t[F_{yy}(w + w_0)_{xx} + F_{xx}(w + w_0)_{yy} - 2F_{xy}(w + w_0)_{xy}] = (w_{xxxx} + 2w_{xxyy} + w_{yyyy})D - p \tag{11}$$

where p is the lateral pressure, t is plate thickness, and D is the bending stiffness of the plate,

$$D = \frac{Et^3}{12(1 - \nu^2)} \tag{12}$$

The condition for strain compatibility can be derived from the membrane strain equations, Eqs. (5–7). By differentiation and combination of the equations, the plate compatibility equation becomes:

$$\nabla^4 F = E(w_{xy}^2 - w_{xx}w_{yy} + 2w_{0,xy}w_{xy} - w_{0,xx}w_{yy} - w_{0,yy}w_{xx}). \tag{13}$$

The two differential Eqs. (11) and (13) are the von Karman plate equations modified for plates with imperfections. They are of the fourth order and coupled, and therefore not possible to solve in general. Here, the continuous deflection w is replaced by a set of assumed displacement functions. Then, a stress function F that satisfies the compatibility equation must be found. Using the principle of minimum potential energy, the displacement amplitudes is calculated without having to solve the plate differential equation.

2.3. Material law

Since the onset of yielding is taken as the criterion for the ultimate load of the structure, material nonlinearities are not considered. Formulations which include plasticity effects have been developed for unstiffened plates, and reasonable results have been obtained even in the post-critical region. However, numerical integration has to be used when plasticity is included. This reduces the computational efficiency drastically. Isotropic, elastic material is therefore assumed throughout the current work. The material then follows Hooke's law:

$$\sigma_{ij} = C_{ijkl}\varepsilon_{kl} \qquad i,j,k,l = x,y,z \tag{14}$$

where C_{ijkl} is the general linear elastic stiffness tensor. For thin plates it is usual to assume plane stress condition, so that $\sigma_z=\tau_{yz}=\tau_{zx}=0$. We can then simply write:

$$\sigma_x = \frac{\mathrm{E}}{(1+\nu^2)}(\varepsilon_x + \nu\varepsilon_y) \tag{15}$$

$$\sigma_y = \frac{\mathrm{E}}{(1+\nu^2)}(\varepsilon_y + \nu\varepsilon_x) \tag{16}$$

$$\sigma_{xy} = G\gamma_{xy}. \tag{17}$$

The von Mises yield criterion is used to check for yielding:

$$\sigma_{\mathrm{eq}} = \sqrt{\sigma_x^2 + \sigma_y^2 - \sigma_x\sigma_y + 3\sigma_{xy}^2} < \sigma_{\mathrm{f}} \tag{18}$$

where σ_{eq} is the equivalent stress, and σ_{f} is the initial yield stress of the material.

2.4. Staging and incrementation

A stiffened plate may be subjected to a combination of several loads, which may be applied sequentially, proportionally, or by some other scheme. In order to reduce the number of load parameters to one, a piecewise linear load path is prescribed. Each linear part of the load history is called a stage, and the process is therefore

referred to as staging. Within each stage s, the load parameter is varied from 0 to 1. The external forces P_i can then be represented by the single load parameter Λ as:

$$P_i(\Lambda) = P_i^{(s-1)} + \Lambda\,[P_i^{(s)} - P_i^{(s-1)}]. \tag{19}$$

Now only the load parameter Λ enters the equation system as an unknown, and all loads may be calculated from the load parameter after the solution has been obtained. Any desired load history may be approximated by defining a sufficiently large number of load stages.

As will be shown, the potential energy of a plate subjected to large deflections is of the fourth order in the deflection. The equations resulting from the principle of minimum potential energy and the Rayleigh–Ritz method are therefore of the third order in the displacement amplitudes. An incremental solution procedure is applied in order to obtain a linear equation system, and to avoid solving a set of third order equations. Linear equation systems are easily solved, and have a unique solution in contrast to third order systems. Using perturbation theory, as done in [9], a general rate parameter η is defined so that:

$$\dot{A}_{mn} = \frac{\partial A_{mn}}{\partial \eta} \tag{20}$$

$$\dot{\Lambda} = \frac{\partial \Lambda}{\partial \eta}. \tag{21}$$

The rate parameter may be considered as a pseudo-time. With this method, any type of behavior can be handled, including passing limit points and turning points. It means that even unstable phenomenon such as snap-through and snap-back problems can be analysed. The updated displacements and load parameter are calculated as:

$$A_{mn}^{i} = A_{mn}^{i-1} + \eta \dot{A}_{mn}^{i-1} + \frac{1}{2}\eta^2 \ddot{A}_{mn}^{i-1} + \ldots \tag{22}$$

$$\Lambda^{i} = \Lambda^{i-1} + \eta \dot{\Lambda}^{i-1} + \frac{1}{2}\eta^2 \ddot{\Lambda}_{mn}^{i-1} + \ldots \tag{23}$$

where i is the current increment. In principle, the perturbation theory can be applied up to any order. For the unstiffened plate, the energy formulations are derived up to the second order. The second order terms can be considered as an alternative to using equilibrium iterations between the increments. They increase the accuracy and can be used to control the size of the increments in the analysis, as the second order rate represents the curvature of the equilibrium curve. It is found, however, that the first order approximation gives sufficient accuracy for small increments. This will be demonstrated by numerical examples, which are all based on first order incrementation.

Defining the perturbation parameter so that the increments are taken as specified steps along the equilibrium curve in the load-displacement space, the following relation must be satisfied:

$$\Delta\Lambda^2 + \Delta q_{mn}^2 = \Delta\eta^2. \tag{24}$$

Summation over all *mn* are implied, and q_{mn} is the displacement amplitudes made non-dimensional with respect to some geometry parameter, such as the plate thickness:

$$q_{mn} = \frac{A_{mn}}{t}. \tag{25}$$

The scaling is necessary to make the equations dimensionally consistent. By taking the limit as the increments go towards zero, the following relation is found:

$$\dot{\Lambda}^2 + \dot{q}_{mn}^2 = 1. \tag{26}$$

2.5. Solving the equations

Applying the principle of minimum potential energy on rate form, the problem is reduced to a system of (M·N) linear equations with (M·N+1) unknowns. The unknowns are the M·N displacement rate amplitudes $\dot{A}_{mn}$ and the load rate parameter $\dot{\Lambda}$. The last equation necessary to solve the equation system is Eq. (26). The equation system can be written on matrix form as:

$$\mathbf{K}\dot{\mathbf{A}} + \mathbf{G}\dot{\Lambda} = \mathbf{0} \tag{27}$$

where the **K**-matrix may be interpreted as an incremental stiffness matrix, while the **G**-vector can be interpreted as an incremental load vector. The equation system is solved as follows:

$$\dot{\mathbf{A}} = -\dot{\Lambda}\mathbf{K}^{-1}\mathbf{G} = \dot{\Lambda}\mathbf{D} \tag{28}$$

where **D** is defined as $\mathbf{D} = \mathbf{K}^{-1}\mathbf{G}$ and has the elements d_{mn}. Substituting **D** into Eq. (26) gives:

$$\dot{\Lambda}^2(d_1^2 + d_2^2 + \ \ldots\ + d_{MN}^2 + t^2) = t^2 \tag{29}$$

$$\Rightarrow \dot{\Lambda} = \pm \frac{t}{\sqrt{d_1^2 + d_2^2 + \ \ldots\ + d_{MN}^2 + t^2}}. \tag{30}$$

The displacement rate amplitudes are then found as $\dot{A}_{mn} = \dot{\Lambda} d_{mn}$. The reason for the ± in Eq. (30) is that by specifying an arc length increment along the equilibrium curve there will always be two possible solutions, one in the direction of positive traversal and one in the direction of negative traversal. The solution corresponding to positive traversal is found using the angle criterion, which is based on the assumption that the equilibrium curve is smooth. Hence, the angle between the tangents to the curve in two consecutive increments should be a small number. Numerically, this can be implemented by calculating the angles α_+ and α_- corresponding to the + and − sign in Eq. (30) above:

$$\alpha_+ = \arccos\left[\dot{\Lambda}_+(\dot{\Lambda}_{i-1} + \frac{d_{mn}\dot{A}_{mn,i-1}}{t^2})\right] \tag{31}$$

$$\alpha_{-} = \arccos\left[\dot{\Lambda}_{-}(\dot{\Lambda}_{i-1} + \frac{d_{mn}\dot{A}_{mn,i-1}}{t^2})\right]. \tag{32}$$

The correct sign of the load rate parameter is $\dot{\Lambda}_{+}$ if α_{+} is the smaller angle, and $\dot{\Lambda}_{-}$ if α_{-} is the smaller angle.

3. Simply supported plate

As a first step towards developing a combined plate/stiffener model, the simply supported plate is studied (Fig. 2). The approach followed is the same as that of Levy [10], but in addition geometrical imperfections are accounted for using Marguerre's plate theory. Shear force is also included as an additional load case. This problem was also solved by Ueda et al. [4] using an incremental Galerkin method.

3.1. Assumptions

The edges of the plate are assumed to be free to move in-plane, but forced to remain straight (Fig. 3). This restriction represents the effect of the neighboring plates that will support the plate in a larger structure. The condition for simply supported edges is:

$$\begin{aligned} &w = 0 \quad \text{at all edges} \\ &w_{yy} + \nu w_{xx} = 0 \quad \text{at } y = 0,b \\ &w_{xx} + \nu w_{yy} = 0 \quad \text{at x} = 0,a. \end{aligned} \tag{33}$$

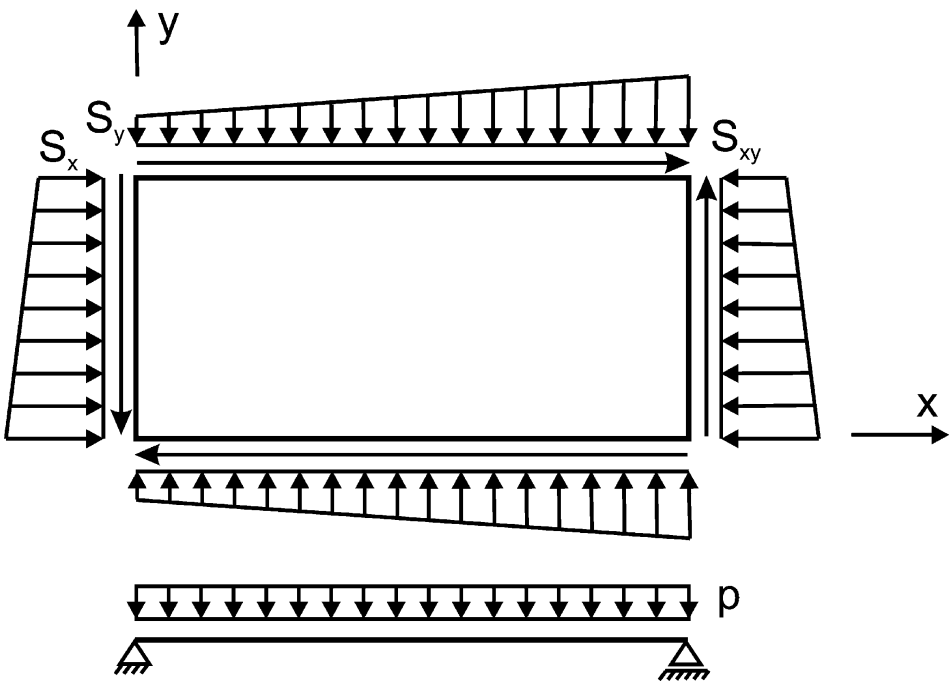

Fig. 2. Unstiffened simply supported plate.

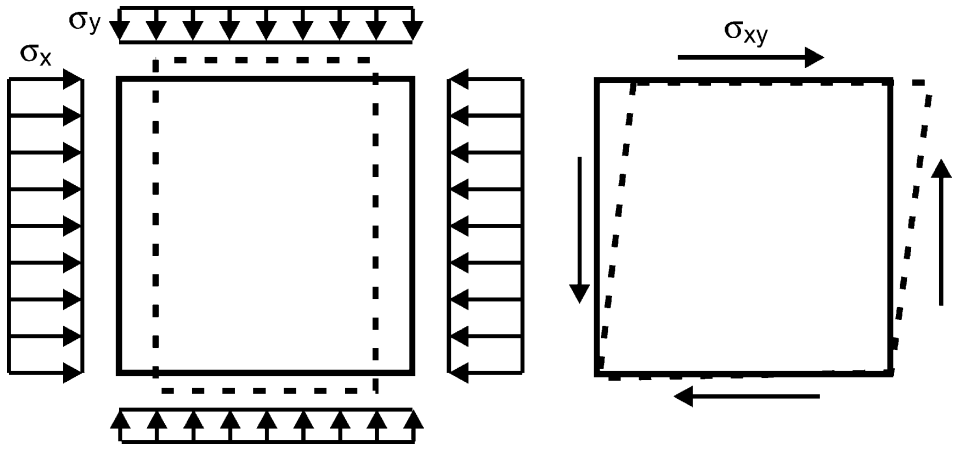

Fig. 3. Boundary conditions for unstiffened plate.

These conditions are satisfied by taking the additional and initial deflections as double Fourier series:

$$w_s = \sum_{m=1}^{M_s}\sum_{n=1}^{N_s} A_{mn}^s \sin\left(\frac{m\pi x}{a}\right)\sin\left(\frac{n\pi y}{b}\right) \tag{34}$$

$$w_{s0} = \sum_{m=1}^{M_s}\sum_{n=1}^{N_s} B_{mn}^s \sin\left(\frac{m\pi x}{a}\right)\sin\left(\frac{n\pi y}{b}\right) \tag{35}$$

where s is used to indicate the sine-mode, in contrast to the cosine-mode which will be introduced later. Initial deflection is included in order to avoid bifurcation problems, and because all plates in the real world have a certain degree of out-of-plane imperfection resulting from the fabrication process. A conservative approach is to set the imperfection shape equal to the eigenmode of the plate. Alternatively, the measured imperfection w_i in a plate may be represented by w_{s0} by calculating the Fourier coefficients:

$$B_{mn}^s = \frac{4}{ab}\int_a\int_b w_i(x,y)\sin\left(\frac{m\pi x}{a}\right)\sin\left(\frac{n\pi y}{b}\right)\mathrm{d}y\mathrm{d}x. \tag{36}$$

Perfect plates can be analysed as a limiting case by specifying a very small initial deflection.

In order to satisfy strain compatibility, a stress function F must be found using the assumed displacements, so that the plate compatibility equation is satisfied. It is assumed to have the following form:

$$F^s = -\frac{P_x y^2}{2bt} - \frac{P_y x^2}{2at} - \frac{P_{xy} xy}{t} + \sum_{0}^{2M_s}\sum_{0}^{2N_s} f_{mn}^s \cos\left(\frac{m\pi x}{a}\right)\cos\left(\frac{n\pi y}{b}\right). \tag{37}$$

The stress function coefficients f_{mn}^s satisfying the compatibility equation are found by substitution of the above equations into the compatibility equation. The result is:

$$f^s_{mn} = \frac{E}{4\left(m^2\frac{b}{a} + n^2\frac{a}{b}\right)^2}\sum_{rspq} b^s_{rspq}(A^s_{rs}A^s_{pq} + A^s_{rs}B^s_{pq} + A^s_{pq}B^s_{rs}) \tag{38}$$

where $f^s_{0,0}$ is defined as zero, and the coefficients b^s_{rspq} are integer numbers given as

$$b^s_{rspq} = rspq + r^2q^2 \text{ if } \begin{cases} \pm(r-p) = m, s + q = n \\ r + p = m \pm (s-q) = n \end{cases} \tag{39}$$

$$b^s_{rspq} = rspq - r^2q^2 \text{ if } \begin{cases} r + p = m, s + q = n \\ \pm(r-p) = m \pm (s-q) = n. \end{cases} \tag{40}$$

From the stress function, the stress components $\sigma_x = F^s_{yy}$, $\sigma_y = F^s_{xx}$, and $\sigma_{xy} = -F^s_{xy}$ are found by differentiation. It can be shown that the above stress function satisfies not only the compatibility equation, but also the boundary conditions of the plate. The integrated stress resultant in any cross-section equals the external load, while the integrated end shortening is constant over the edges. Knowing the stresses, the internal potential energy can be calculated as outlined in the following.

3.2. Potential of internal energy

The internal energy in the plate can be divided into two contributions, one due to membrane stretching of the middle plane of the plate, and one due to bending about the middle plane. The energy expressions resulting for the membrane part will be presented as an example of the procedure followed, while the other contributions are left out due to space limitations. Further details may be found in [11].

Using the stress function, the membrane energy can be expressed as:

$$U_m = \frac{t}{2E}\int_0^a\int_0^b [(F^s_{xx} + F^s_{yy})^2 - 2(1+\nu)(F^s_{xx}F^s_{yy} - (F^s_{xy})^2)]\mathrm{d}y\mathrm{d}x. \tag{41}$$

Introducing the assumed form of the stress function, integration over the plate area can be carried out analytically. The result is:

$$U_m = \frac{t}{2E}\left[\frac{P_x^2 a}{bt^2} + \frac{P_y^2 b}{at^2} - 2\nu\frac{P_xP_y}{t^2} + \frac{ab}{4}\pi^4\sum_0^{2M_s}\sum_0^{2N_s}(f^s_{mn})^2\left(\frac{m^2}{a^2} + \frac{n^2}{b^2}\right)^2\right. \tag{42}$$

$$\left. + \frac{ab}{2}\pi^4\sum_0^{2M_s}(f^s_{m0})^2\left(\frac{m}{a}\right)^4 + \frac{ab}{2}\pi^4\sum_0^{2N_s}(f^s_{0n})^2\left(\frac{n}{a}\right)^4\right].$$

It is seen that the membrane energy is proportional to the displacement amplitudes A^s_{mn} to the fourth power, since f^s_{mn} is quadratic in A^s_{mn}. By differentiation, the minimum membrane energy is:

$$\frac{\partial U_m}{\partial A^s_{fg}} = \frac{abt}{4E}\pi^4 \sum_0^{2M_s}\sum_0^{2N_s} \frac{\partial f^s_{mn}}{\partial A^s_{fg}} f^s_{mn}\left(\frac{m^2}{a^2}+\frac{n^2}{b^2}\right)^2 + \frac{abt}{2E}\pi^4 \sum_0^{2M_s} \frac{\partial f^s_{m0}}{\partial A^s_{fg}} f^s_{m0}\left(\frac{m}{a}\right)^4 + \frac{abt}{2E}\pi^4 \sum_0^{2N_s} \frac{\partial f^s_{0n}}{\partial A^s_{fg}} f^s_{0n}\left(\frac{n}{b}\right)^4. \tag{43}$$

This expression is of third order in A^s_{mn}, since the coefficients f^s_{mn} are quadratic and $\frac{\partial f^s_{mn}}{\partial A^s_{fg}}$ are linear in A^s_{mn}. The rate of minimum membrane energy is:

$$\left(\frac{\partial \dot{U}_m}{\partial A^s_{fg}}\right) = \frac{abt}{4E}\pi^4 \sum_0^{2M_s}\sum_0^{2N_s} \left[\frac{\partial f^s_{mn}}{\partial A^s_{fg}} \dot{f}^s_{mn} + \left(\frac{\partial \dot{f}^s_{mn}}{\partial A^s_{fg}}\right) f^s_{mn}\right]\left(\frac{m^2}{a^2}+\frac{n^2}{b^2}\right)^2 + \frac{abt}{2E}\pi^4 \sum_0^{2M_s} \left[\frac{\partial f^s_{m0}}{\partial A^s_{fg}} \dot{f}^s_{m0} + \left(\frac{\partial \dot{f}^s_{m0}}{\partial A^s_{fg}}\right) f^s_{m0}\right]\left(\frac{m}{a}\right)^4 + \frac{abt}{2E}\pi^4 \sum_0^{2N_s} \left[\frac{\partial f^s_{0n}}{\partial A^s_{fg}} \dot{f}^s_{0n} + \left(\frac{\partial \dot{f}^s_{0n}}{\partial A^s_{fg}}\right) f^s_{0n}\right]\left(\frac{n}{b}\right)^4. \tag{44}$$

The potential energy due to bending is:

$$U_b = \frac{D}{2}\int_0^a\int_0^b [(w^s_{xx} + w^s_{yy})^2 - 2(1-\nu)(w^s_{xx}w^s_{yy} - (w^s_{xy})^2)]\mathrm{d}y\mathrm{d}x. \tag{45}$$

The integration over the plate area can be carried out analytically by introducing the assumed form of the displacements. The result is not given here, but the bending energy is proportional to the square of the displacement amplitudes, and gives a constant contribution to the incremental plate stiffness. The incremental bending stiffness therefore only needs to be calculated once, in contrast to the incremental membrane stiffness which must be calculated for each new increment.

3.3. Potential of external loads

The potential of external in-plane compressive forces is calculated as external force multiplied with displacement:

$$T_p = P_x\Delta u + P_y\Delta v \tag{46}$$

where Δu and Δv are the end shortenings of the plate in the x- and y-direction, respectively. These are calculated using the Marguerre's plate theory [Eqs. (5)(6)], which means that:

$$\Delta u = \int_0^a \left(\varepsilon_x - \frac{1}{2}w^2_{s,x} - w_{s0,x}w_{s,x}\right)\mathrm{d}x \tag{47}$$

$$\Delta v = \int_0^b \left(\varepsilon_y - \frac{1}{2} w_{s,y}^2 - w_{s0,y} w_{s,y} \right) \mathrm{d}y. \tag{48}$$

Carrying out the integration, it is found that the potential of external loads consists of two parts. One part contributes to the incremental load vector **G**, and is proportional to the displacement. The other part contributes to the incremental stiffness matrix **K**, and is proportional to the external load parameter λ, defined in Eq. (19).

The potential of external energy due to the shear flow $P_{xy}=\tau_{xy}t$ is:

$$T_\tau = P_{xy} \int_0^a \int_0^b (u_y + v_x) \mathrm{d}y \mathrm{d}x. \tag{49}$$

Rearranging the shear strain expression, Eq. (7), we get:

$$T_\tau = P_{xy} \int_0^a \int_0^b (\gamma_{xy} - w_x w_y - w_{0,x} w_y - w_x w_{0,y}) \mathrm{d}y \mathrm{d}x. \tag{50}$$

where the effect of the γ_{xy}-term must be zero due to static equilibrium. The lateral pressure p does not lead to any additional stress in the plate since the direction of the pressure is out-of-plane. The contribution to the potential of external energy is:

$$T_{lp} = -\int_0^a \int_0^b p w \mathrm{d}y \mathrm{d}x. \tag{51}$$

The lateral pressure gives a constant contribution to the incremental load vector, but no contribution to the incremental stiffness matrix.

If the in-plane loads are linearly varying, the external stress is written:

$$S_x(y) = S_x^1 + (S_x^2 - S_x^1)\frac{y}{b} \tag{52}$$

$$S_y(x) = S_y^1 + (S_y^2 - S_y^1)\frac{x}{a}. \tag{53}$$

The external energy is then calculated using the modified stress function:

$$F^s = -S_x^1 \frac{y^2}{2} - (S_x^2 - S_x^1)\frac{y^3}{6b} - S_y^1 \frac{x^2}{2} - (S_y^2 - S_y^1)\frac{x^3}{6a} - \frac{P_{xy} xy}{t} + \sum_0^{2M_s} \sum_0^{2N_s} f_{mn}^s \cos\left(\frac{m\pi x}{a}\right) \cos\left(\frac{n\pi y}{b}\right). \tag{54}$$

3.4. Total rate of minimum potential energy

The total rate of minimum potential energy is found by adding the contributions from internal and external energy:

$$\left(\frac{\partial \dot{\Pi}}{\partial A_{fg}}\right) = \left(\frac{\partial \dot{U}_m}{\partial A_{fg}}\right) + \left(\frac{\partial \dot{U}_b}{\partial A_{fg}}\right) + \left(\frac{\partial \dot{T}_P}{\partial A_{fg}}\right) + \left(\frac{\partial \dot{T}_\gamma}{\partial A_{fg}}\right) + \left(\frac{\partial \dot{T}_{lp}}{\partial A_{fg}}\right). \tag{55}$$

This results in a linear equation system, on the form of Eq. (27). Solving this equation system, a set of displacement rate amplitudes $\dot{A}_{mn}$ is found, which are used to calculate the next increment in the analysis.

3.5. Verification

Some numerical examples of application of the proposed model are given. The results are compared with analyzes performed with the nonlinear FEM program ABAQUS [12]. For all calculations, an elastic modulus of E=208,000 MPa is used. The plates are modeled using 4 node double curved general-purpose shell elements, S4R. The sources of inaccuracy in the proposed model are drift from the correct equilibrium curve due to the incrementation, and difference between correct and assumed displacement shape. The former is controlled by specifying sufficiently small values of the perturbation parameter, while the latter is controlled by specifying sufficiently large number of terms in the assumed displacement functions. A suitable set of parameters can be found by convergence tests. The initial deflections are set to a small value, since the intention is only to compare the computational model with nonlinear FEM, and not to represent actual fabricated plates.

To the left in Fig. 4, the load-deflection response of a quadratic plate subjected to biaxial loading is shown. Proportional loading is used, and the magnitude of the load is the same in both directions. The number of terms in the deflection function is 3×3, and it is seen that the correspondence is good. The right plot shows the load-

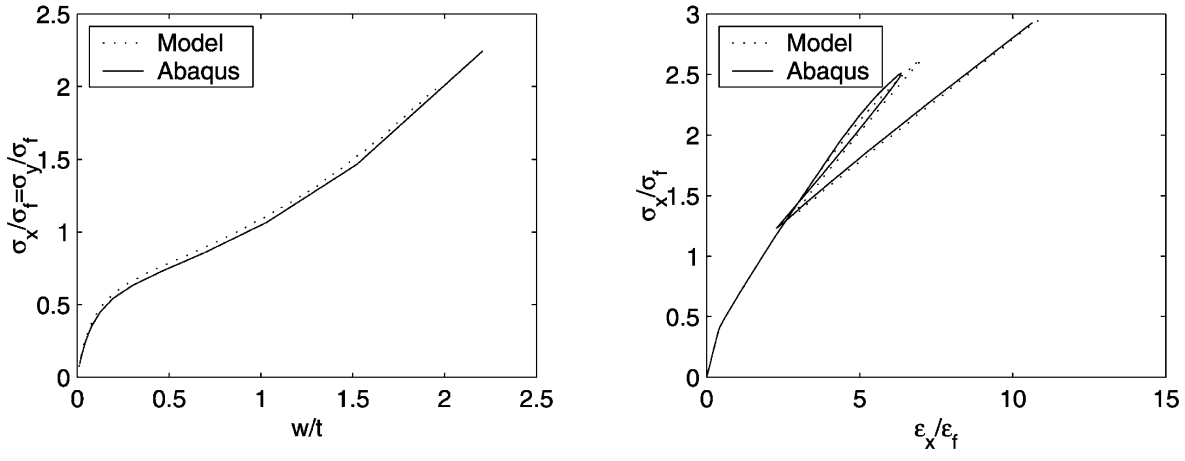

Fig. 4. Deflection at midpoint under biaxial loading for 1.0×1.0×0.026 plate(left) and snap-back under axial loading for 1.68×0.98×0.011 plate(right).

end shortening response of a rectangular plate subjected to axial loading, using 8×8 deflection terms in the calculation model. The snap-back in the postbuckling region is provoked by specifying an initial deflection mode which is different from the preferred one, leading to violent mode snapping. It should be noted that the snap-back occurs very far out in the postbuckling region, and is therefore of more academic than practical interest. The intention is to demonstrate that such complex responses is well treated with the perturbation method used, even if only first order terms are included in the formulations. In Fig. 5, the load-deflection response for a quadratic plate subjected to lateral pressure and shear loading is shown. The number of terms used is 3×3 for both cases. The accuracy of the calculations is good, and the efficiency is very high.

4. Clamped plate

The edges of a plate are considered as clamped if the surrounding structure is strong enough to prevent rotation of the edges. Clamped-like conditions may also occur due to the applied loads. Lateral pressure may cause a plate to deflect symmetrically about a stiffener, and thereby causing a clamped deflection mode. Here, it is assumed that the longitudinal edges of the plate are clamped, while the transverse edges are taken as simply supported, Fig. 6. The number of half waves will usually be greater than one in the longitudinal direction, due to the effect of axial compression and the plate aspect ratio, and the effect of the lateral pressure on the deflection shape is therefore less significant.

4.1. Assumptions

The condition for clamped longitudinal edges is written:

$$\begin{aligned} &w = 0 \quad \text{at all edges} \\ &w_y = 0 \quad \text{at } y = 0,b \\ &w_{xx} + \nu w_{yy} = 0 \quad \text{at } x = 0,a. \end{aligned} \tag{56}$$

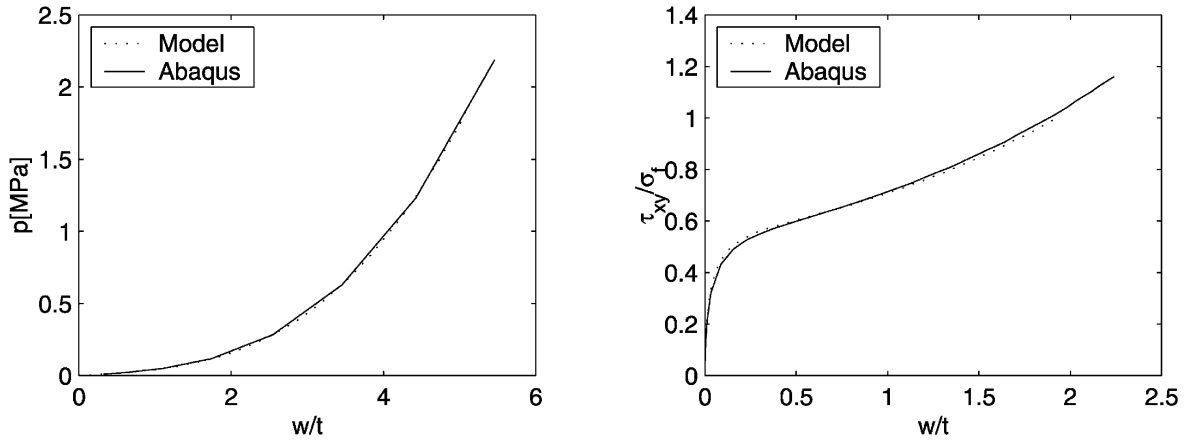

Fig. 5. Deflection at midpoint under lateral pressure(left) and shear loading(right) for 1.0×1.0×0.009 plate.

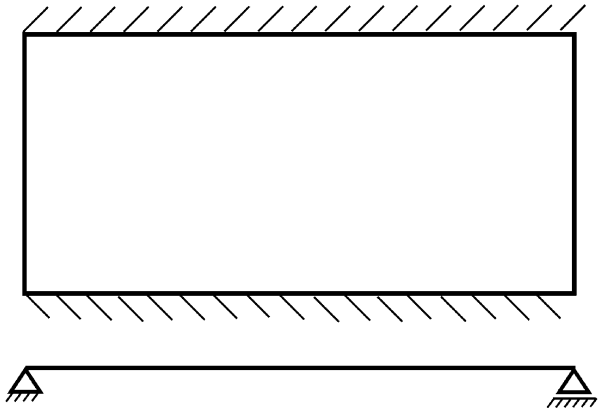

Fig. 6. Clamped plate.

One way to handle clamped edges is to use the same displacement functions as for the simply supported plate, and to add a rotational spring along the clamped edges. The essential boundary conditions are then satisfied, and the clamped condition can be analyzed by applying a very stiff spring. Good results are obtained with this method, but the number of terms required in the displacement function is large. The displacement shape is estimated reasonably well with less terms, but the bending moment distribution requires more terms. This is because the bending moment resulting from a sine-series is zero along the edges, while the bending moment for a clamped plate attains its maximum value at the edges.

Better results are achieved using cosine-terms. The following displacement shape is used:

$$w_c = \sum_{m=1}^{M_c}\sum_{n=1}^{N_c} \frac{A^c_{mn}}{2}\sin\left(\frac{m\pi x}{a}\right)\left(1-\cos\left(\frac{2n\pi y}{b}\right)\right) \tag{57}$$

$$w_{c0} = \sum_{m=1}^{M_c}\sum_{n=1}^{N_c} \frac{B^c_{mn}}{2}\sin\left(\frac{m\pi x}{a}\right)\left(1-\cos\left(\frac{2n\pi y}{b}\right)\right). \tag{58}$$

The above expressions represent a far better approximation to the clamped condition than the sine-terms, and good results may be obtained with only a few degrees of freedom, e.g. 2 or 3. In the following, a stress function is derived for these displacements, and potential energy-expressions are established.

4.2. Stress function

The approach used for deriving the stress function for the clamped plate is the same as for the simply-supported plate. The result is:

$$F^c = -\frac{P_x y^2}{2bt} - \frac{P_y x^2}{2at} - \frac{P_{xy} xy}{t} + \sum_{0}^{2M_c}\sum_{0}^{2N_c} f^c_{mn}\cos\left(\frac{m\pi x}{a}\right)\cos\left(\frac{2n\pi y}{b}\right). \tag{59}$$

The coefficients f^c_{mn} are

$$f^c_{mn} = \frac{E}{4\left(m^2\frac{b}{a} + 4n^2\frac{a}{b}\right)^2}\sum_{rspq} b^c_{rspq}(A^c_{rs}A^c_{pq} + A^c_{rs}B^c_{pq} + A^c_{pq}B^c_{rs}) \tag{60}$$

where $f^c_{0,0}$ is defined as zero, and the coefficients b^c_{rspq} are:

$$b^c_{rspq} = \begin{cases} 2r^2q^2 & \text{if } \pm(r-p) = m, q = n \\ -2r^2q^2 & \text{if } r+p = m, q = n \\ -rspq - r^2q^2 & \text{if } \pm(r-p) = m, s+q = n \\ rspq + r^2q^2 & \text{if } r+p = m, \pm(s-q) = n \\ -rspq + r^2q^2 & \text{if } r+p = m, s+q = n \\ rspq - r^2q^2 & \text{if } \pm(r-p) = m, \pm(s-q) = n \end{cases} . \tag{61}$$

4.3. Potential energy

The same expressions as before is used for calculation of membrane and bending energy. By substitution of the new displacement function and stress function, analytical integration can be carried out. The potential of external in-plane compressive forces, and the potential of lateral pressure, is also calculated as for the simply supported plate.

For the shear force, substituting the assumed displacements into the energy expression used previously gives:

$$T_\tau = P_{xy}\int_0^a\int_0^b (\gamma_{xy} - w_{c,x}w_{c,y} - w_{c0,x}w_{c,y} - w_{c,x}w_{c0,y})\mathrm{d}y\mathrm{d}x \tag{62}$$

$$= 0 \tag{63}$$

The reason is that the cosine-terms are always symmetric, and they are therefore not able to describe shear deformation. For shear force analysis, it is necessary to include sine-terms in the deflection shape. One approach is the one described previously, where a pure sine-series is used together with a very stiff spring. An even better strategy is to use cosine-terms and sine-terms in combination. This is done for the combined plate/stiffener-model presented in the next section, and it is therefore not further described here.

4.4. Verification

In Fig. 7, the load-end shortening response for a plate with clamped longitudinal edges subjected to axial loading is shown. Calculations using sine-terms as well as

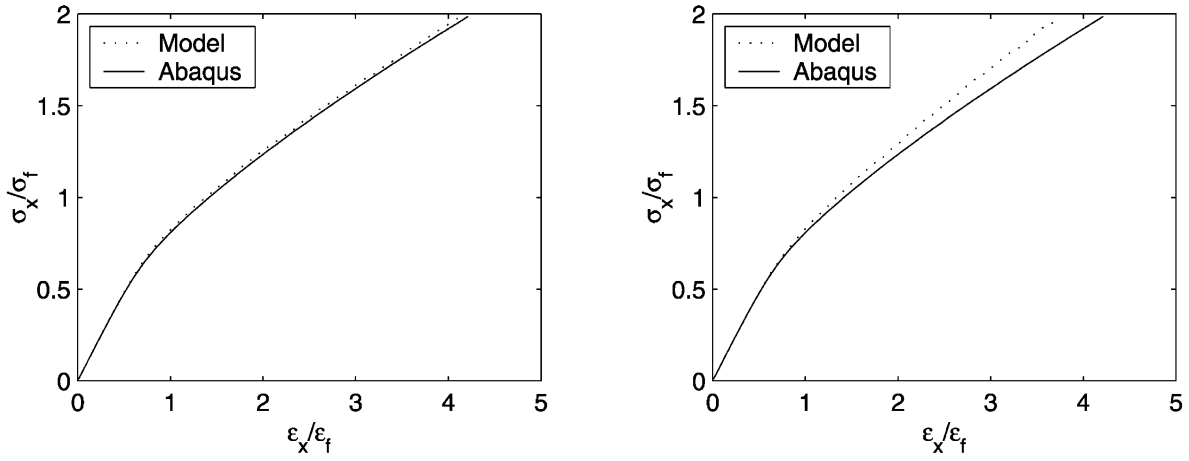

Fig. 7. Load-shortening for 1.0×1.0×0.013 clamped plate under axial loading calculated using 2×3 cosine-terms(left) and 2×11 sine-terms(right).

cosine-terms are shown. In the left plot, good accuracy is obtained with only 2×3 cosine-terms, while in the right plot 2×11 sine-terms have been used.

5. Local stiffened plate model

Now the local buckling of a plate with an attached stiffener is considered. By local buckling, it is meant that the plate, the web and the flange may deform locally, but the stiffener as a whole may not deflect laterally. In other words, the connection between the plate and the stiffener is fixed in the vertical direction (Fig. 8). Lateral support is also provided by transverse girders. The stiffener is assumed to be of the open profile type, which means it may be a flat bar, angle bar, tee-bar, or bulb profile.

5.1. Plate deflection

The stiffener acts as a rotational spring on the plate. As a result, the boundary condition for a plate between two stiffeners is somewhere in between simply supported and clamped. For most stiffened plates the web is quite slender compared to

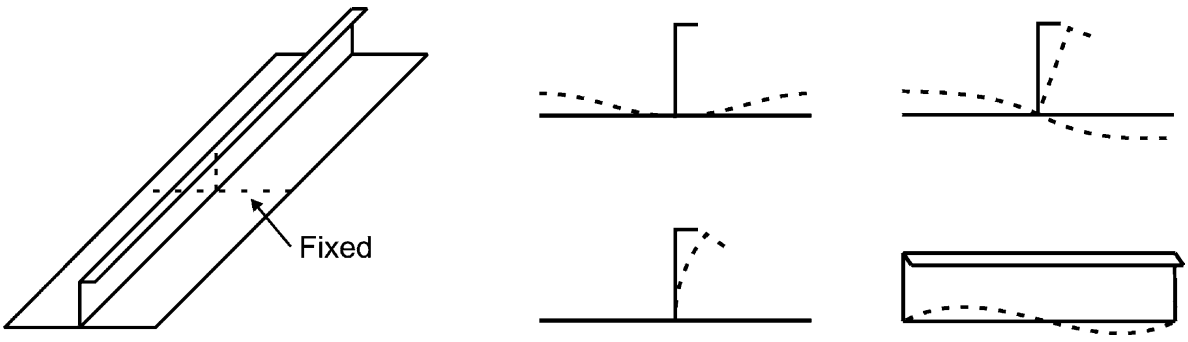

Fig. 8. Local model with assumed deflection modes.

the plate itself, so that the situation is quite close to that of simply support. The clamped mode becomes more important for stronger webs and under influence of lateral pressure. In order to include the possibility of all types of plate deflections in the range from simply supported to fully clamped, it is necessary to assume the deflection shape as a combination of sine-terms and cosine-terms. Hence, the assumed displacement pattern for additional and initial deflection is:

$$w = w_s + w_c \tag{64}$$

$$w_0 = w_{s0} + w_{c0} \tag{65}$$

where s and c denotes sine and cosine mode deflection, respectively. Both w_s and w_c are as given in the previous sections.

Combining the sine-deflection and the cosine-deflection affects the strain compatibility. Due to coupling terms in the strain compatibility equation, a new stress function must be derived. The total stress function is now written as:

$$F = F^0 + F^s + F^c + F^{sc} \tag{66}$$

where:

$$F^0 = -\frac{P_x y^2}{2bt} - \frac{P_y x^2}{2at} - \frac{P_{xy} xy}{t} \tag{67}$$

$$F^s = \sum_0^{2M_s} \sum_0^{2N_s} f^s_{mn} \cos\left(\frac{m\pi x}{a}\right) \cos\left(\frac{n\pi y}{b}\right) \tag{68}$$

$$F^c = \sum_0^{2M_c} \sum_0^{2N_c} f^c_{mn} \cos\left(\frac{m\pi x}{a}\right) \cos\left(\frac{2n\pi y}{b}\right) \tag{69}$$

$$F^{sc} = \sum_0^{M_s + M_c} \sum_0^{N_s + 2N_c} f^{sc}_{mn} \cos\left(\frac{m\pi x}{a}\right) \sin\left(\frac{n\pi y}{b}\right). \tag{70}$$

The coefficients f^s_{mn} and f^c_{mn} are as given before, while f^{sc}_{mn} are:

$$f^{sc}_{mn} = \frac{E}{4\left(m^2\frac{b}{a} + n^2\frac{a}{b}\right)^2} \sum_{rspq} b^{sc}_{rspq} (A^s_{rs} A^c_{pq} + A^s_{rs} B^c_{pq} + A^c_{pq} B^s_{rs}) \tag{71}$$

where $f^{sc}_{0,0}$ is defined as zero, and the coefficients b^{sc}_{rspq} are:

$$b^{sc}_{rspq} = 2rspq + 2r^2q^2 + \frac{1}{2}s^2p^2 \quad \text{if} \quad \begin{cases} p + r = m, 2q - s = n \\ \pm(p - r) = m, s + 2q = n \end{cases} \tag{72}$$

$$b^{sc}_{rspq} = 2rspq - 2r^2q^2 - \frac{1}{2}s^2p^2 \quad \text{if} \quad \begin{cases} p + r = m, 2q + s = n \\ \pm(p - r) = m, 2q - s = n \end{cases} \tag{73}$$

$$b^{sc}_{rspq} = -2rspq + 2r^2q^2 + \frac{1}{2}s^2p^2 \quad \text{if} \quad \begin{cases} p + r = m, s-2q = n \\ \pm (p-r) = m, s-2q = n. \end{cases} \tag{74}$$

5.2. Stiffener deflection

The displacement shape chosen for the stiffener is:

$$v = \frac{z}{h}\sum_{m=1}^{M_s} V_{1m}\sin\left(\frac{m\pi x}{a}\right) + \left(1-\cos\left(\frac{\pi z}{2h}\right)\right)\sum_{m=1}^{M_s} V_{2m}\sin\left(\frac{m\pi x}{a}\right). \tag{75}$$

The first part represents rigid torsion of the stiffener, while the second involves bending of the web (Fig. 8). Both involve torsion and bending of the flange. Other displacement functions may be used for the stiffener, and increasingly better results could be obtained if more terms were included. For stiffeners with very heavy flanges, for instance, buckling may occur in the web without a high degree of distortion of the flange. In such cases, it may be beneficial to use a deflection pattern which allows for web deflections without flange distortion. However, eigenvalue analysis including several other deflection shapes have shown that the two mode shapes suggested above are the most important for practical cases. In order to limit the number of degrees of freedom in the model, only these two are included. Requiring rotation continuity at the plate-stiffener connection, as discussed in the next section, eliminates the variables V_{1m}, and leaves the additional variables V_{2m}. The total number of degrees of freedom is therefore $(M_sN_s+M_cN_c+M_s)$. For comparison, a deformation plot from FEM-analysis for an angle bar stiffener subjected to axial loading is shown in Fig. 9.

5.3. Transverse continuity

The requirement for rotational continuity at the plate-stiffener connection is:

$$\left.\frac{\partial v}{\partial z}\right|_{z=0} = -\left.\frac{\partial w}{\partial y}\right|_{y=0}. \tag{76}$$

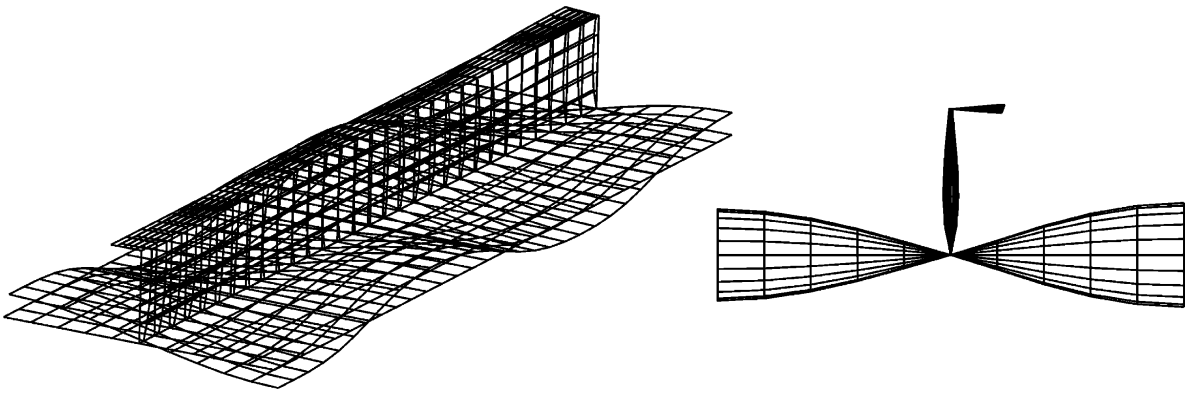

Fig. 9. Deformation plot for axial loading from ABAQUS for angle bar.

The minus-sign is due to the definition of the right-handed coordinate system. For the plate a positive deflection gives a positive rotation, while for the stiffener a positive deflection gives a negative rotation. Substituting the deflection shapes for the plate and the stiffener we find that:

$$V_{1m} = -h\sum_n \frac{n\pi}{b} A^{\mathrm{s}}_{mn}. \tag{77}$$

The deflection modes V_{2m} has no rotation at the plate-stiffener connection, and does therefore not enter the continuity equations. This is also the case for the cosine-deflection modes A^{c}_{mn} of the plate.

5.4. Longitudinal continuity

When considering the plate and the stiffener as one member, longitudinal continuity also has to be fulfilled. The transverse members, i.e. girders or bulkheads, are assumed to enforce the same displacement in the longitudinal direction for the stiffener as for the plate. If the displacement is constant over the height of the stiffened plate, while the stiffness is not, it follows that the applied external stress must be unevenly distributed between the two members. Since the stiffness of each member is changing during buckling, the ratio of external load carried by each is initially unknown, and the force distribution needs to be included in the energy formulations.

For the unstiffened plate, the external stress was assumed to be directly transferred into the plate, and did not enter the equilibrium equations. Turning to the stiffened plate, the membrane stress is divided into a part due to deflection, σ^a, and a part due to the external force, σ^f:

$$\sigma^{\mathrm{p}} = \sigma^{\mathrm{p},a} + \sigma^{\mathrm{p},f} \tag{78}$$

$$\sigma^{\mathrm{s}} = \sigma^{\mathrm{s},a} + \sigma^{\mathrm{s},f} \tag{79}$$

where p denotes plate, and s stiffener. Both the deflection part and the force part are now unknowns. It is still assumed that the membrane stress due to the external force is constant over each member, but in general unevenly distributed between the two.

Expressions for the membrane strains due to external force may be derived using two requirements. The first is that the end shortening takes a constant value over the cross-section, so that the plate displacement equals the stiffener displacement, and the second is that the internal stress resultant equals the external force:

$$Du^{\mathrm{p}} = Du^{\mathrm{s}} \tag{80}$$

$$N^{\mathrm{p}}_x + N^{\mathrm{s}}_x = -P_x. \tag{81}$$

The minus-sign is because the external force P_x is defined as positive in compression, in contrast to the internal forces. The end shortenings in the plate may be written

$$Du^{\mathrm{p}} = \int_a \left(\varepsilon^{\mathrm{p},f}_x + \varepsilon^{\mathrm{p},a}_x - \frac{1}{2} w_x^2 - w_{0,x} w_x \right) \mathrm{d}x \tag{82}$$

$$= a\varepsilon_x^{p,f} + Du^{p,a} \tag{83}$$

$$Dv^p = \int_b \left(\varepsilon_y^{p,f} + \varepsilon_y^{p,a} - \frac{1}{2} w_y^2 - w_{0,y} w_y \right) dy \tag{84}$$

$$= b\varepsilon_y^{p,f} + Dv^{p,a} \tag{85}$$

while the internal stress resultants are

$$N_x^p = \int_b \int_t (\sigma_x^{p,f} + \sigma_x^{p,a}) dz dy \tag{86}$$

$$= bt\sigma_x^{p,f} \tag{87}$$

$$N_y^p = \int_a \int_t (\sigma_y^{p,f} + \sigma_y^{p,a}) dz dx \tag{88}$$

$$= at\sigma_y^{p,f}. \tag{89}$$

The integrated effect of the deflection membrane stress must be zero due to static equilibrium, and does therefore fall out of the equations. In the transverse direction, we get

$$\varepsilon_y^{p,f} = -(1-\nu^2)\frac{P_y}{atE} - \nu\varepsilon_x^{p,f} \tag{90}$$

which gives:

$$N_x^p = Ebt\left(\varepsilon_x^{p,f} - \frac{\nu P_y}{atE} \right). \tag{91}$$

A fundamental assumption introduced for the stiffener is that the longitudinal displacement is constant over the height of the stiffener, so that

$$u_x^s = \varepsilon_x^{s,f} + \varepsilon_x^{s,a} - \frac{1}{2} v_x^2 = \text{constant}. \tag{92}$$

This assumption is based on the fact that the length of the stiffener is usually much larger than the height, and it has been verified by non-linear FEM-analysis for some practical cases. Since $\varepsilon_x^{s,f}$ is also assumed to be constant, we can simply choose

$$u_x^s = \varepsilon_x^{s,f} \tag{93}$$

$$\varepsilon_x^{s,a} = \frac{1}{2} v_x^2. \tag{94}$$

The end shortening becomes

$$Du^s = \int_0^a u_x dx \tag{95}$$

$$= a\varepsilon_x^{s,f} \tag{96}$$

and the stiffener stress resultant

$$N_x^s = \frac{1}{a}\int_{V_s}(\sigma_x^{s,f} + \sigma_x^{s,a})\mathrm{d}V_s \tag{97}$$

$$= A_s E\varepsilon_x^{s,f} + \frac{E}{a}\int_{V_s}\varepsilon_x^{s,a}\mathrm{d}V_s \tag{98}$$

where V_s and A_s are stiffener volume and cross-sectional area, respectively. In the last relation, the one-dimensional Hooke's law, $\sigma_x = E\varepsilon_x$, is used. It is thus assumed that no membrane stress develops in the stiffener in the vertical direction. Using the continuity condition $Du^p = Du^s$ it is found that:

$$\varepsilon_x^{s,f} = \varepsilon_x^{p,f} + \frac{Du^{p,a}}{a}. \tag{99}$$

Now considering force equilibrium in the longitudinal direction, we write:

$$-P_x = N_x^s + N_x^p \tag{100}$$

$$= A_s E\left(\varepsilon_x^{p,f} + \frac{Du^{p,a}}{a}\right) + \frac{E}{2a}\int_{V_s} v_x^2\mathrm{d}V_s + Ebt\left(\varepsilon_x^{p,f} - \frac{\nu P_y}{atE}\right). \tag{101}$$

Rearranging, an expression for the plate membrane strain due to the external force is found:

$$\varepsilon_x^{p,f} = \frac{-P_x a + \nu P_y b - Du^{p,a} E A_s - \dfrac{E}{2}\displaystyle\int_{V_s} v_x^2\mathrm{d}V_s}{aE(bt + A_s)}. \tag{102}$$

The strain $\varepsilon_x^{p,f}$ is here expressed by the load variables P_x and P_y, and by the displacement variables A_{mn}^s, A_{mn}^c, and V_{2m} through $Du^{p,a}$ and v_x. The strain will therefore come out as part of the solution to the whole problem.

5.5. Internal potential energy

The plate bending energy is due to the combined effect of the sine-deflection and the cosine-deflection. It is expressed:

$$U_b^p = \frac{D}{2}\int_{-a/2}^{a_u}\int_{-b/2}^{b_u}(w_{s,xx}^2 + w_{s,yy}^2 + 2w_{s,xx}w_{s,yy} + w_{c,xx}^2 + w_{c,yy}^2$$

$$+ 2w_{c,xx}w_{c,yy} + 2w_{s,xx}w_{c,xx} + 2w_{s,yy}w_{c,yy} + 2w_{s,xx}w_{c,yy} + 2w_{c,xx}w_{s,yy})\mathrm{d}y\mathrm{d}x \tag{103}$$

where a_u and b_u are upper limits of integration. From the resulting expressions, it can be seen that integrating to $3a/2$ and $3b/2$ instead of $a/2$ and $b/2$ eliminates the coupling terms between odd and even half wave numbers. The integration is therefore taken over two plate breadths and lengths, and the resulting expressions divided by four. This ensures that the continuity of the plating is accounted for. In FEM-analysis this is done by prescribing symmetry or anti-symmetry conditions at the edges, depending on the anticipated deflection mode. Using the current model and performing the integration as explained, no assumptions have to be made beforehand regarding the deflection mode. The deflection shape will automatically adjust itself to the one which is most beneficial with respect to the plate geometry and loading.

The web bending energy is:

$$U_b^w = \frac{D_w}{2}\int_{-a/2}^{a_u}\int_0^h [(v_{xx} + v_{zz})^2 - 2(1-\nu)(v_{xx}v_{zz} + v_{xz}^2)]\mathrm{d}z\mathrm{d}x. \tag{104}$$

The bending stiffness coefficients are found by inserting the expression for V_{1m} found from the continuity condition, integrating over the area, and differentiating with respect to the rate and displacement amplitudes.

The flange bending energy is:

$$U_b^f = \frac{EI_f}{2}\int_{-a/2}^{a_u}(v_{xx}|_{z=h})^2\mathrm{d}x + \frac{GJ_f}{2}\int_{-a/2}^{a_u}(v_{xz}|_{z=h})^2\mathrm{d}x \tag{105}$$

where the first part is due to in-plane bending of the flange, and the second is due to torsion of the flange. EI_f is the bending stiffness and GJ_f the torsional stiffness of the flange. As for the web, the bending stiffness coefficients are found by inserting the expression for V_{1m} and differentiating with respect to the rate and displacement amplitudes.

The plate membrane energy is

$$U_m^{\mathrm{p}} = \frac{E}{2(1-\nu)^2}\int_{V_p}((\varepsilon_x^{\mathrm{p},f})^2 + (\varepsilon_y^{\mathrm{p},f})^2 + 2\nu(\varepsilon_x^{\mathrm{p},f})(\varepsilon_y^{\mathrm{p},f}))\mathrm{d}V_{\mathrm{p}} \tag{106}$$

$$+ \frac{E}{2(1-\nu)^2}\int_{V_p}\left((\varepsilon_x^{\mathrm{p},a})^2 + (\varepsilon_y^{\mathrm{p},a})^2 + 2\nu(\varepsilon_x^{\mathrm{p},a})(\varepsilon_y^{\mathrm{p},a}) + \frac{1-\nu}{2}\gamma_{xy}^2\right)\mathrm{d}V_{\mathrm{p}}$$

$$= U_m^{\mathrm{p},f} + U_m^{\mathrm{p},a}. \tag{107}$$

The coupling between $\varepsilon^{\mathrm{p},a}$ and $\varepsilon^{\mathrm{p},f}$ is zero, since $\varepsilon^{\mathrm{p},f}$ is constant and the integral of

$\varepsilon^{p,a}$ over the plate area is zero. The deflection part $U_m^{p,a}$ of the membrane energy for the plate may be written

$$U_m^{p,a} = U_m^{p,s} + U_m^{p,c} + U_m^{p,sc} \tag{108}$$

where $U_m^{p,s}$ is the membrane energy due to sine-deflection, $U_m^{p,c}$ is that due to cosine-deflection, and $U_m^{p,sc}$ is due to coupling effects.

The external force part, $U_m^{p,f}$, can be found by taking the constant membrane strain outside the integration, and substituting the expression for $\varepsilon_y^{p,f}$. It is found that $\varepsilon_y^{p,f}$ cancels out:

$$U_m^{p,f} = \frac{abtE}{2(1-\nu)^2}[(\varepsilon_x^{p,f})^2 + (\varepsilon_y^{p,f})^2 + 2\nu(\varepsilon_x^{p,f})(\varepsilon_y^{p,f})] \tag{109}$$

$$= \frac{1}{2}abtE(\varepsilon_x^{p,f})^2. \tag{110}$$

The stiffener membrane energy is

$$U_m^s = \frac{E}{2}\int_{V_s}(\varepsilon_x^{s,f} + \varepsilon_x^{s,a})^2 dV_s \tag{111}$$

$$= \frac{EV_s}{2}(\varepsilon_x^{s,f})^2 + \frac{E}{2}\int_{V_s}(\varepsilon_x^{s,a})^2 dV_s + E\varepsilon_x^{s,f}\int_{V_s}\varepsilon_x^{s,a} dV_s. \tag{112}$$

By substitution of all parameters and integrating, U_m^s is found as a function of the unknown load parameter and displacement amplitudes. Since the energy expressions are of the fourth order the derivations are tedious, but relatively straightforward.

5.6. External potential energy

Using the displacements calculated for the plate and stiffener in combination, the external energy due to in-plane compression can be calculated directly. The external energy due to shear force and lateral pressure needs some special consideration. The sine-terms in the deflection shape are anti-symmetric about x=0 and y=0. This means that integrating the external shear energy directly gives zero contribution, since only sine-terms are included in the longitudinal direction. The chosen deflection shape is therefore not able to describe the continuous deflection of two neighboring plates under the action of shear loading correctly. An approximate solution may be obtained by neglecting the interaction between the plates, and looking at each plate individually. This means that the plate energy is integrated between (0−a), and then multiplied with a factor 2. This is a conservative approach, since the restraining effect of the two plates on each other is neglected. However, FEM-analyses have shown that the restraining effect under pure shear loading is quite small. In the transverse direction, only the plate area between the stiffeners is included. Hence, the shear energy is calculated as:

$$T_\tau = -2P_{xy}\int_0^a\int_0^b (w_{s,x}w_{s,y} + w_{s,0x}w_{s,y} + w_{s,x}w_{s,0y} + w_{c,x}w_{c,y} + w_{c,0x}w_{c,y} + w_{c,x}w_{c0,y} + w_{s,x}w_{c,y} + w_{s0,x}w_{c,y} + w_{s,x}w_{c0,y} + w_{c,x}w_{s,y} + w_{c0,x}w_{s,y} + w_{c,x}w_{s0,y})\mathrm{d}y\mathrm{d}x. \quad (113)$$

A similar consideration has to be made regarding calculation of external energy due to lateral pressure. When integrating the sine-terms in the longitudinal direction, the $(-a/2-0)$ part will always cancel the $(0-a/2)$ part. As for the shear-force, the integration is therefore taken between (0−a), and multiplied by two. Physically, this means that the plate continuity at the transverse member is not fulfilled, which makes the model less stiff than the real structure. However, the lateral pressure is believed to have the largest influence on the deflection shape in the transverse direction. The cosine-terms included are capable of describing the transverse deflection shape due to the pressure, and the integration can therefore be taken directly between $(-b/2-3b/2)$. The potential of external energy due to lateral pressure is therefore taken as:

$$T_\mathrm{p} = -2\int_0^a\int_{-b/2}^{3b/2} pw\mathrm{d}y\mathrm{d}x. \quad (114)$$

5.7. Verification

Computations have been performed on a variety of stiffener geometries for verification of the proposed model. Results are presented for a flat bar, an angle bar and a tee bar stiffener, with dimensions given in Table 1. Results for axial and transverse compression are shown for each stiffener in Figs. 10–12. The initial deflection for each stiffener is taken as the eigenmode, with an amplitude of 1.0 mm. The real imperfections present in actual stiffened plates are usually larger and more complex, but such considerations are not an issue in the current work. The results are compared with FEM-calculations, and the accuracy is good. Increasingly better results are obtained with more terms included in the deflection function and smaller increments. For the geometries and load conditions presented, deflection in the cosine-mode is small, and good results are obtained with sine-terms included only.

Table 1
Stiffener dimensions

Stiffener	a	b	t	h	t_w	b_f	t_f	σ_f
Flat bar	4.75	0.91	0.018	0.325	0.020			355
Angle bar	2.73	0.85	0.0165	0.350	0.012	0.100	0.017	355
Tee bar	4.335	0.814	0.020	0.475	0.012	0.200	0.025	325

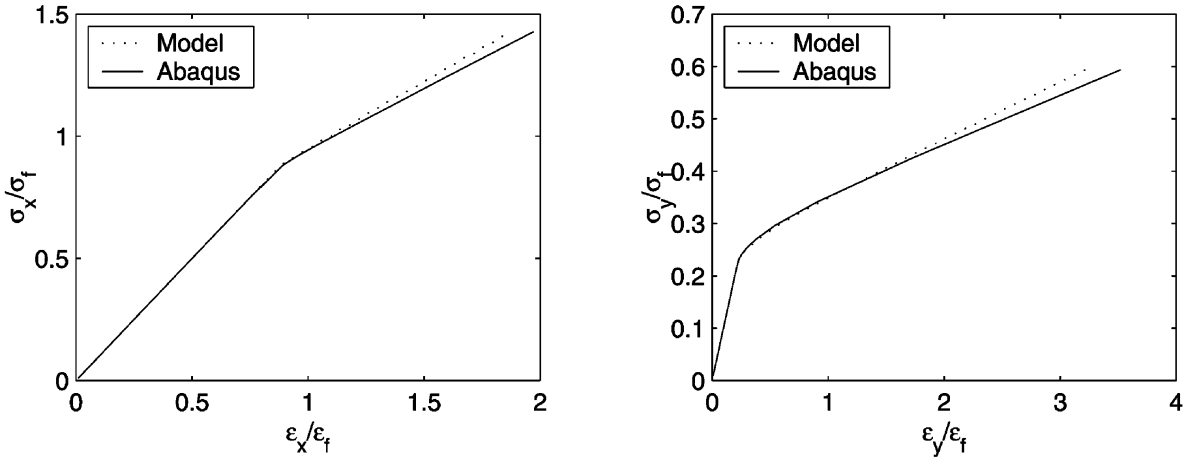

Fig. 10. Flat bar under axial loading using 5×1 terms(left) and transverse loading using 7×3 terms(right).

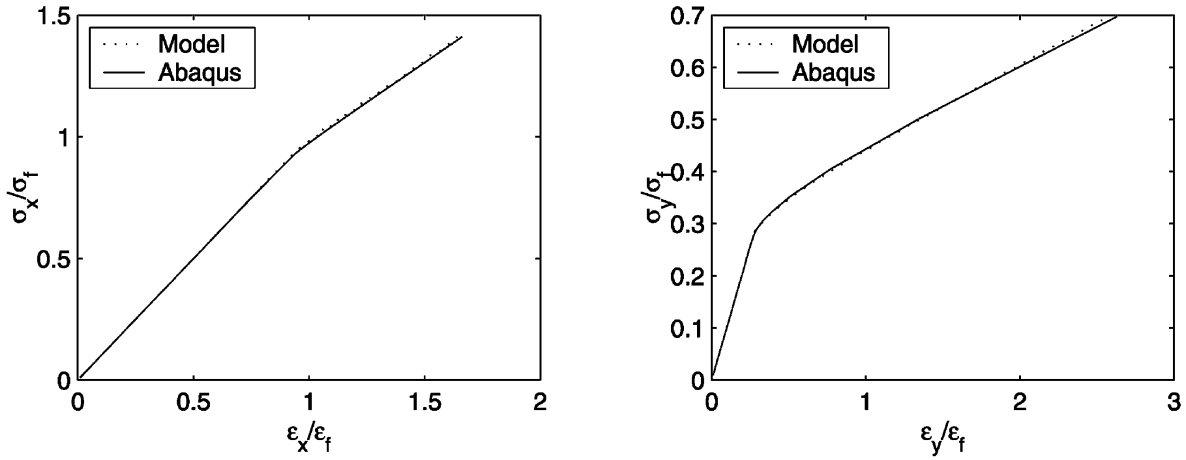

Fig. 11. Angle bar under axial loading using 3×1 terms(left) and transverse loading using 5×3 terms(right).

6. Estimation of design ultimate limit state load

A first yield approach is used for estimation of the collapse load using the local buckling model presented. First yield has often been applied to assess the critical load in design formulations, such as in the DNV Classification Note. Using a column model together with a first yield criterion has commonly been referred to as the Perry-Robertson approach. Local buckling effects are implicitly accounted for by specifying an effective plate breadth which is less than the full breadth.

First yield is a sound design criterion, because yielding will give unwanted permanent deformations in the structure. Also, the reserve capacity after the onset of yielding is usually moderate, and is questionable to utilize in design. It is found that for predominantly axial loading, collapse is mainly governed by the membrane stress in the flange. For predominantly transverse loading, however, collapse is often triggered

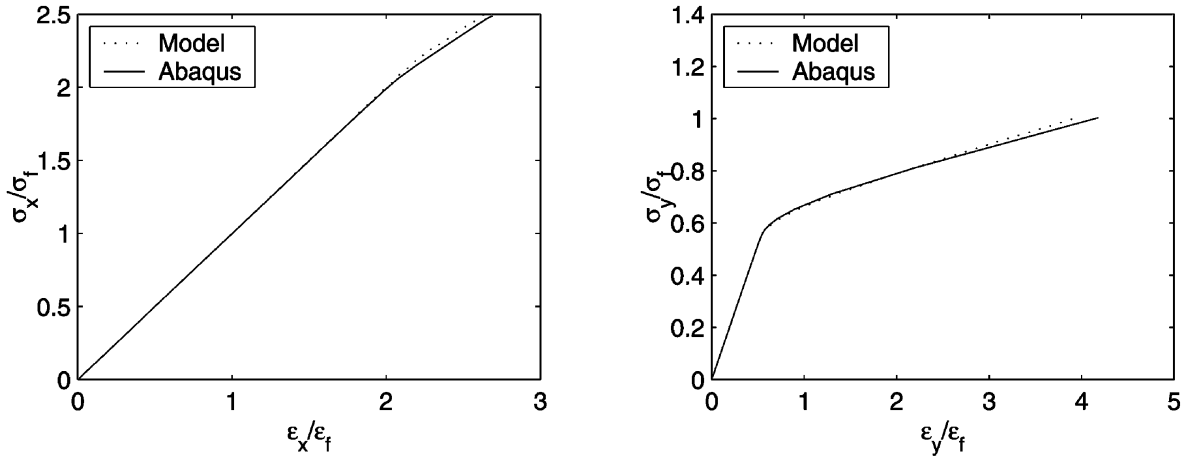

Fig. 12. Tee bar under axial loading using 5×1 terms(left) and transverse loading using 7×3 terms(right).

by large bending stresses developing along the longitudinal edges. Collapse may even occur before the equivalent membrane stress reaches yield. Consequently, different collapse criteria must be used for different load conditions, and the effect of bending stresses must be accounted for. This can be done by using a membrane-bending capacity interaction curve.

One way to account for some of the reserve capacity after the onset of yielding, is the approach used for instance in [5] for unstiffened plates. The plate is then divided into a mesh, considered to consist of several fibers. When yielding starts in the outer fibers, they loose their strength, and the total stiffness is reduced accordingly. Yielding will then spread to more and more fibers, until the panel collapses. In this way, the panel may be able to sustain some additional loading after the first yield. This approach is beneficial especially for analysis of aluminum panels. The effect of reduced yield stress in the heat affected zones may then be included in the calculations very efficiently. Although yielding may occur quite early in the HAZ-zones, the rest of the structure may be able to sustain further loading.

Interaction curves for biaxial loading obtained using the first yield criterion is presented for the angle bar stiffener, and compared with collapse loads obtained from fully nonlinear FEM-analyses, Fig. 13. In the FEM-analysis, linear elastic-linear plastic material is specified, with a strain hardening parameter E_T=1000 MPa. The results are presented as examples of application of the proposed model, but it is emphasized that more work is needed in order to establish reliable collapse criteria for all relevant load conditions. In the left plot, a criterion using first yield in the outer fibers is applied. In the right plot, bending stress is accounted for using a membrane-bending interaction curve. Also, the flange is removed at first yield, and the remaining structure loaded further up until yielding occurs in the plate. It is seen that this gives some additional capacity, and reduces the gap between the model predictions and the FEM-results.

For most ship panels the global buckling load is much higher than the local buckling load, and often the global buckling load is well above the squash load. Panels

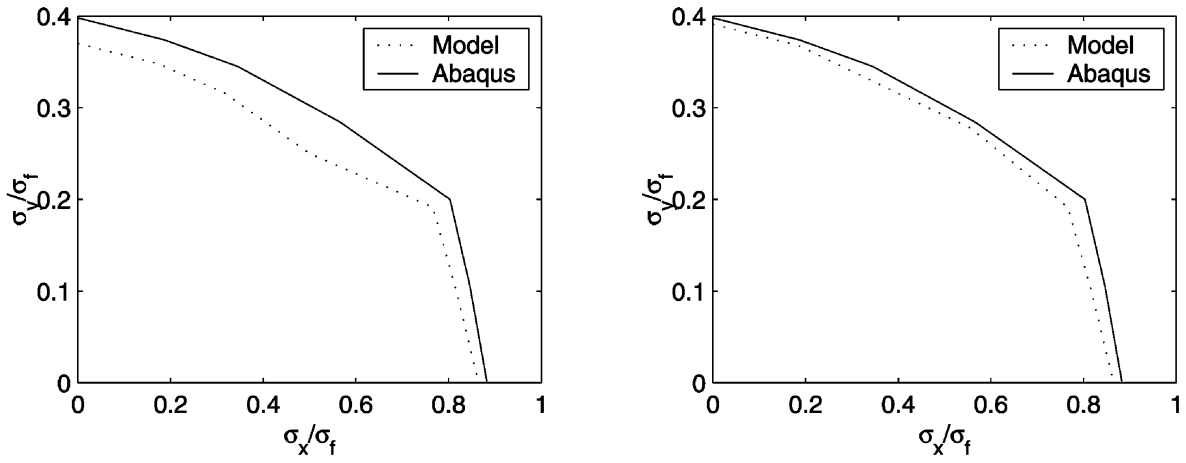

Fig. 13. Interaction curves for angle bar using first yield criterion(left) and modified first yield criterion(right).

with global buckling load close to the local buckling load may experience very unstable response in the postbuckling region, and it is therefore good design practice to ensure that the global buckling load is well above the local buckling load. Due to geometrical imperfections, however, global deflections start to grow immediately when load is applied. The global deflection will therefore produce stresses that must be accounted for when controlling first yield in the panel. A simplified method for including moderate global buckling effects is to add the global stresses directly to the local one, and check the total stress against yield in each step. Using a column model for assessing the global deflection of the stiffened plate with imperfection, the global stress may easily be calculated for each step in the local model. Assuming linear response for the global deflection, the deflection amplitude δ_m at the load P for a structure with initial deflection amplitude δ_{m0} and Euler buckling load P_E is:

$$\delta_m = \frac{P}{P_E - P}\delta_{m0}. \tag{115}$$

Using this simple formulae, the global deflection and thereby the global stresses corresponding to each load level P in the local analysis, may be calculated and added to the local stresses.

7. Concluding remarks

A computational model for analysis of local buckling and postbuckling of stiffened panels has been derived. The motivation was to develop a tool that is more accurate than existing design codes, and more efficient than nonlinear finite element methods. The model is formulated using large deflection plate theory and energy principles. Any combination of biaxial in-plane compression or tension, shear, and lateral pressure may be analysed. The procedure is semi-analytical in the sense that all energy formulations are derived analytically, while a numerical method is used for solving

the resulting set of equations, and for incrementation of the solution. Load–deflection curves produced by the proposed model are compared with results from nonlinear FEM. Good correspondence is achieved, and the efficiency of the calculations is high.

The ultimate strength of panels may be estimated by checking the stress in certain critical points at each increment. Using the von Mises yield criterion, the onset of yielding can be taken as the collapse load for design purposes. This is conservative, and a sound design approach. Examples of capacity interaction curves are presented for biaxial loading for a stiffened plate. Further work is needed in order to establish reliable collapse criteria for all relevant load conditions. For some cases, it is beneficial to account for some of the reserve capacity after first yield by simplified assumptions. This is especially true for aluminum panels including HAZ-zones, and this topic will be considered in more detail in future work. The present local model is suitable for buckling analysis of a wide range of stiffened panels, as the global buckling load of stiffened panels is usually very high. If necessary, global stresses resulting from global deflection may be calculated easily using linear theory, and added to the local stresses for each load level.

8. Acknowledgments

Thanks to Dr Eivind Steen at DNV for valuable discussions. The study has been performed with support from the Norwegian Research Council and DNV.

References

[1] Buckling strength analysis, DNV classification note 30.1. 1995.
[2] Hughes O, Ma M. Elastic tripping analysis of asymmetrical stiffeners. Computers and Structures 1996;60(3):369–89.
[3] Fujikubo M, Yao T. Elastic local buckling strength of stiffened plate considering plate/stiffener interaction and welding residual stress. Marine Structures 1999;12(9):543–64.
[4] Ueda Y, Rashed SMH, Paik JK. An incremental galerkin method for plates and stiffened plates. Computers and Structures 1987;27(1):147–56.
[5] Paik J, Thayamballi A, Lee S, Kang S. A semi-analytical method for the elastic-plastic large deflection analysis of welded steel or aluminium plating under combined in-plane and lateral pressure loads. Thin-Walled Structures 2001;39:125–52.
[6] Washizu K. Variational methods in elasticity and plasticity, 2nd ed. Oxford: Pergamon Press, 1975.
[7] Marguerre K. Die mittragende breite der gedruckten platte. 1937 Luftfahrtsforschung.
[8] Timoshenko SP, Gere JM. Theory of plates and shells, 2nd ed. New York: McGraw-Hill, 1959.
[9] Steen E. Application of the perturbation method to plate buckling problems. Research report in mechanics 98-1, University of Oslo, 1998.
[10] Levy S. Bending of rectangular plates with large deflection. Report 737, NACA, 1937.
[11] Byklum E. Ultimate strength analysis of stiffened steel and aluminium panels using semi-analytic methods. PhD thesis, Norwegian University of Science and Technology, 2002.
[12] Hibbitt, Karlsson and Sorensen. ABAQUS, user manual, version 5.8. 1994.